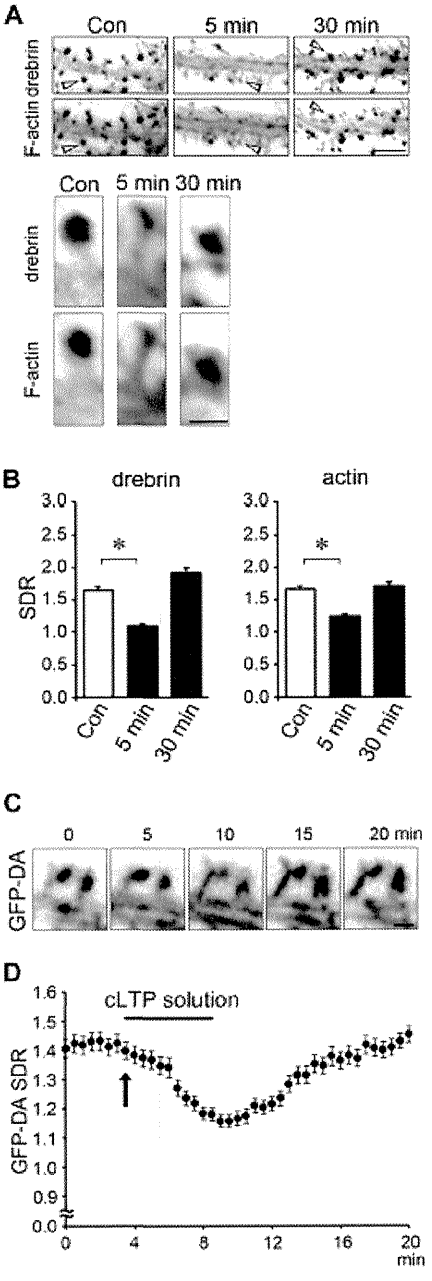

Figure 3. Chemical LTP (cLTP) stimulation induces the exodus and re-entry of DA-actin. (**A**) Neurons (21 DIV) were stimulated with a buffer containing 0 μM Mg^{2+}, 200 μM glycine, 20 μM bicuculline, 1 μM strychnine and 0.5 μM TTX (cLTP stimulation) for 3 min and then fixed 5 or 30 min after stimulation. The fixed cells were double-labeled for drebrin and F-actin. Scale bars, 5 μm and 1 μm in upper and lower panels, respectively. The lower panels show the higher-magnification images of the spines (indicated by arrow heads) in the upper panels. (**B**) Bar graphs represent the spine-dendrite ratios (SDRs) for drebrin and actin. cLTP stimulation significantly decreased the drebrin and actin SDRs at 5 min ($n = 30$ cells; $p < 0.01$, Student's t test). Error bars represent s.e.m. (**C, D**) We transfected 7-DIV neurons with a GFP-drebrin A (GFP-DA)-expressing vector and performed time-lapse imaging at 21 DIV. Scale bar, 1 μm. (**C**) shows the GFP-DA images at 0, 5, 10, 15 and 20 min after the start of the time-lapse recording. The neurons were stimulated with cLTP solution from 3.5 min (indicated by an arrow) to 8.5 min. In (**D**), closed circles represent data obtained at 30-sec intervals. Error bars represent s.e.m. ($n = 7$ neurons). The GFP-DA SDR began to decrease soon after cLTP stimulation. When the stimulation was stopped, the GFP-DA SDR began to increase and recovered to control levels within 10 min.
doi:10.1371/journal.pone.0085367.g003

actin in dendritic spines was similar for both with and without glutamate stimulation (photomicrographs in Fig. 6B). However, quantitative analysis showed that EGTA treatment significantly increased both the drebrin and actin SDRs compared with control neurons. Following the extracellular Ca^{2+} chelation, glutamate stimulation failed to induce decreases in drebrin and actin SDRs ($n = 30$ cells; $p = 0.88$ for drebrin SDR, $p = 0.84$ for actin SDR; Student's t test; graphs in Fig. 6B). These data indicate that Ca^{2+} influx is involved in the changes in both DA-actin and non-DA-actin distribution.

Inhibition of L-type voltage-dependent Ca^{2+} channels with 20 μM nifedipine did not block glutamate-induced changes in drebrin and F-actin localization (photomicrographs in Fig. 6C). Quantitative analysis also showed that nifedipine treatment did not inhibit the glutamate-induced decreases in drebrin and actin SDRs. However, in the absence of glutamate stimulation, nifedipine treatment significantly increased the drebrin and actin SDR levels, similar to the results obtained with APV and EGTA treatments (graphs in Fig. 6C). This indicates that voltage-dependent Ca^{2+} channels regulate the accumulation of DA-actin in dendritic spines, but do not regulate the DA-actin exodus. However, we cannot exclude the possibility that the increase of the basal SDR is due to inhibition of voltage-dependent Ca^{2+} channels in the presynaptic terminus.

Inhibition of Ca^{2+} release from intracellular stores with 1 μM thapsigargin [32] did not block glutamate-induced changes in drebrin and F-actin localization (photomicrographs in Fig. 6D). Quantitative analysis showed that thapsigargin neither increased the drebrin and actin SDRs ($n = 30$ cells; $p = 0.99$ for drebrin SDR, $p = 0.50$ for actin SDR; Student's t test) nor blocked the glutamate-induced decreases in drebrin and actin SDRs ($n = 30$ cells; $p < 0.01$, Scheffe's test; graphs in Fig. 6D).

Together, these data indicate that DA-actin exodus is regulated by NMDA receptors, but not by voltage-dependent Ca^{2+} channels. On the other hand, the basal accumulation of DA-actin in dendritic spines is regulated by both NMDA receptors and voltage-dependent Ca^{2+} channels. Ca^{2+} release from intracellular stores is not involved in either the DA-actin exodus or the basal accumulation of DA-actin.

Glutamate-induced DA-actin exodus is also dependent on myosin II ATPase activity

We examined whether myosin II ATPase is involved in the glutamate-induced DA-actin exodus. In the presence of aBL, drebrin localization at dendritic spines was not affected by glutamate stimulation (photomicrographs in Fig. 7), and glutamate stimulation did not induce a decrease in drebrin SDR ($n = 30$ cells; $p = 0.06$, Student's t test; graph in Fig. 7). Interestingly, the actin SDR was slightly, but significantly, decreased upon glutamate stimulation (graph in Fig. 7), although the decrease was not remarkable compared with that in the presence of iBL (Fig. 7). This result indicates that inhibition of myosin II ATPase does not completely block the exodus of F-actin, indicating that a small amount of F-actin other than DA-actin exits dendritic spines in response to glutamate stimulation.

Together, it is indicated that the glutamate-induced as well as the cLTP-induced DA-actin exodus depends on myosin II ATPase, but the glutamate-induced non-DA-actin exodus is at

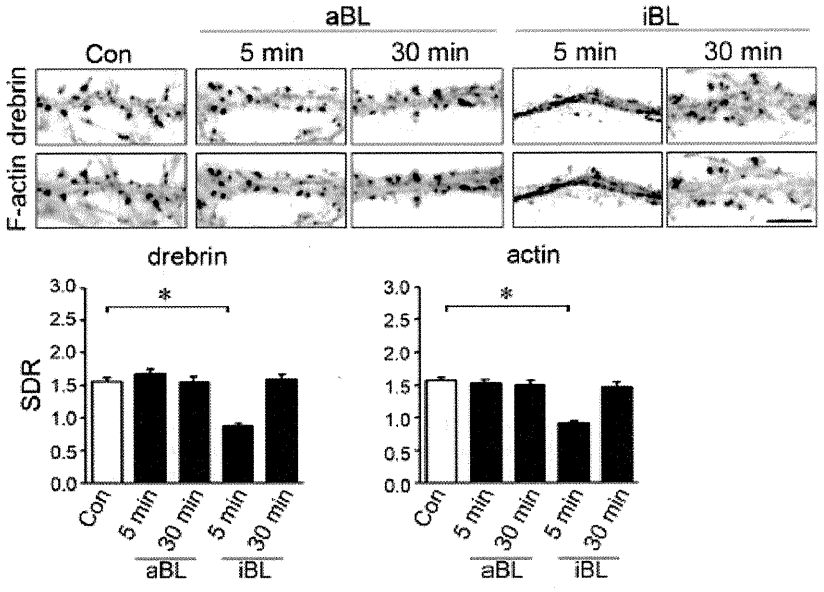

Figure 4. cLTP-induced DA-actin exodus is blocked by an inhibitor of myosin II ATPase. Neurons (21 DIV) were preincubated with 100 μM (S)-(−)-blebbistatin (aBL, the active form of blebbistatin) for 30 min and then stimulated with cLTP solution for 3 min. (R)-(+)-blebbistatin (iBL, the inactive form of blebbistatin) was used as a control. Scale bars, 5 μm. F-actin images indicate that spines kept their structure during the experiment although their shapes were changed. The aBL-treated neurons did not show a decrease in the drebrin and actin SDRs at either 5 min or 30 min after cLTP stimulation (n = 30 cells; Student's test), whereas iBL-treated neurons showed a significant decrease in the drebrin and actin SDRs at 5 min (n = 30 cells; $p<0.01$, Scheffe's test), similar to that observed in control neurons in Fig. 3. Error bars represent s.e.m.
doi:10.1371/journal.pone.0085367.g004

least partly independent of myosin II ATPase. This myosin II-independent loss of non-DA-actin might correspond to the NMDA receptor-independent loss of non-DA-actin shown in Fig. 6A.

The DA-actin exodus is not dependent on phosphorylation of myosin light chain

To examine whether the phosphorylation of myosin light chain (MLC) is involved in the DA-actin exodus, we inhibited myosin

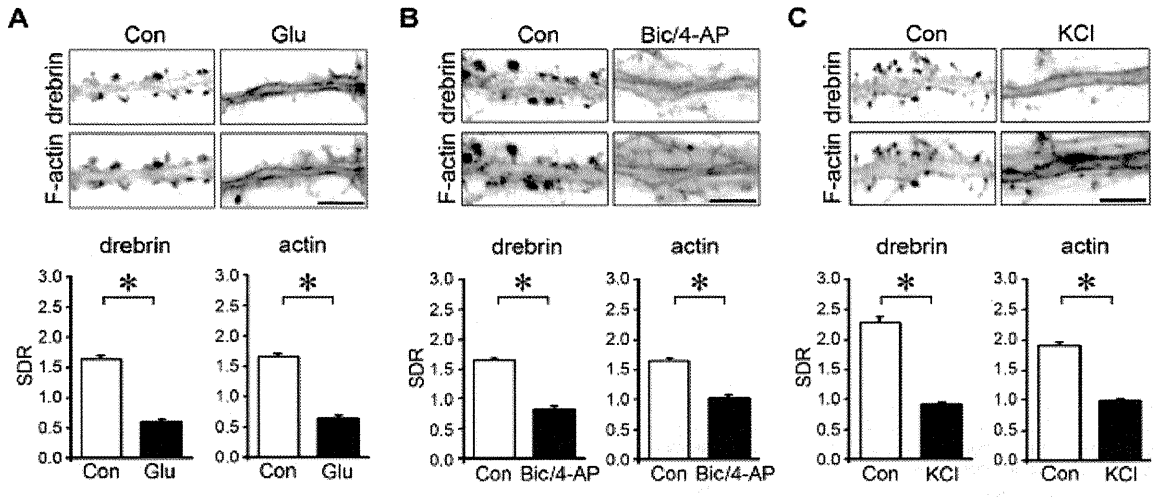

Figure 5. Effects of various excitatory stimulations on DA-actin distribution. Images were obtained from neurons (21 DIV) double-labeled for drebrin and F-actin. Bar graphs represent the spine-dendrite ratios (SDRs) for drebrin and actin. (**A**–**C**) Neurons were stimulated with 100 μM glutamate for 10 min (A), 50 μM bicuculline and 500 μM 4-aminopyridine (Bic/4-AP) for 10 min (B), or 90 mM KCl in Tyrode's solution for 5 min (C). F-actin images indicate that spines kept their structure during the experiment although their shapes were changed. After stimulation, the drebrin and F-actin clusters in the spines disappeared, and a linear staining pattern appeared along the dendrite. Both the drebrin and actin SDRs were significantly decreased (glutamate, n = 170 cells; Bic/4-AP, n = 30 cells; KCl, n = 30 cells; $p<0.01$, Student's *t* test). Note that the control drebrin and actin SDRs in (C) were greater than the other SDRs because Tyrode's solution was used instead of normal medium. Scale bars, 5 μm. Error bars represent s.e.m.
doi:10.1371/journal.pone.0085367.g005

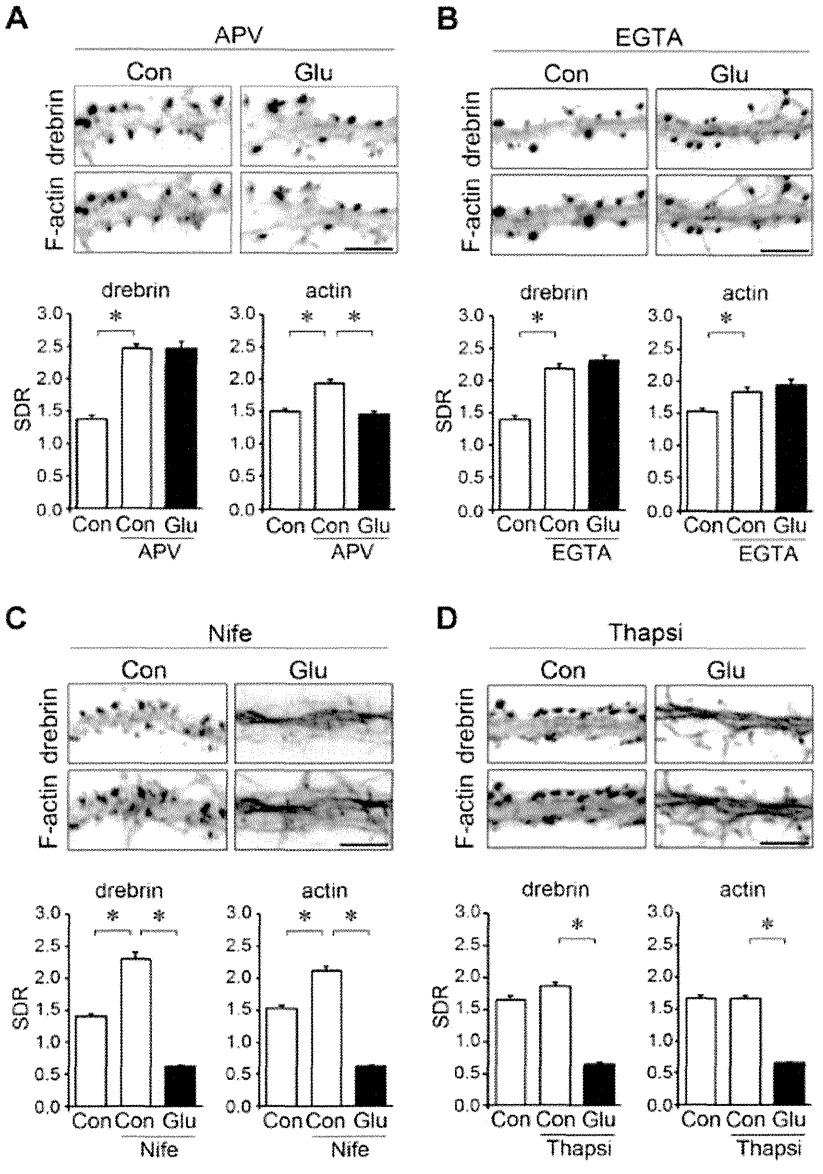

Figure 6. Effects of various inhibitors of Ca^{2+} entry on DA-actin distribution. *Neurons (21 DIV) were incubated in normal medium containing 50 μM APV (A), 20 mM EGTA (B), 20 μM nifedipine (C), or 1 μM thapsigargin (D) for 30 min. The neurons were then stimulated with 100 μM glutamate for an additional 10 min. F-actin images indicate that spines kept their structure during the experiment although their shapes were changed. Scale bars, 5 μm.* **(A)** *APV pretreatment significantly increased both the drebrin and actin SDRs (n = 30 cells; $p<0.01$, Scheffe's test). In the presence of APV, glutamate stimulation significantly decreased the actin SDR (n = 30 cells; $p<0.01$, Student's t test) but not the drebrin SDR (n = 30 cells; p = 0.52, Student's t test).* **(B)** *EGTA significantly increased the drebrin and actin SDRs (n = 30 cells; $p<0.01$, Scheffe's test), and blocked the glutamate-induced decreases in drebrin and actin SDRs (n = 30 cells; Student's t test).* **(C)** *Nifedipine significantly increased the drebrin and actin SDRs (n = 30; $p<0.01$, Scheffe's test), but did not block the glutamate-induced decrease in drebrin and actin SDRs (n = 30; $p<0.01$, Scheffe's test).* **(D)** *Thapsigargin neither increased the drebrin and actin SDRs (n = 30; Student's t test) nor blocked the glutamate-induced decreases in drebrin and actin SDRs (n = 30; $p<0.01$, Scheffe's test). Error bars represent s.e.m.*

doi:10.1371/journal.pone.0085367.g006

light chain kinase (MLCK). When MLCK activity was inhibited with 10 μM ML-7, glutamate stimulation induced the loss of drebrin and F-actin from dendritic spines (photomicrographs in Fig. 8A). Quantitative analysis showed that the ML-7 treatment did not change the drebrin and actin SDR levels compared with control neurons, and did not inhibit the glutamate-induced decreases in the drebrin and actin SDRs (Fig. 8A).

We then inhibited ROCK activity with 1 μM H-1152. In the presence of H-1152, glutamate stimulation induced the loss of drebrin and F-actin from dendritic spines (photomicrographs in Fig. 8B). Quantitative analysis showed that the H-1152 treatment did not change the drebrin and actin SDR levels compared with control neurons, and did not inhibit the glutamate-induced decreases in the drebrin and actin SDRs (Fig. 8B).

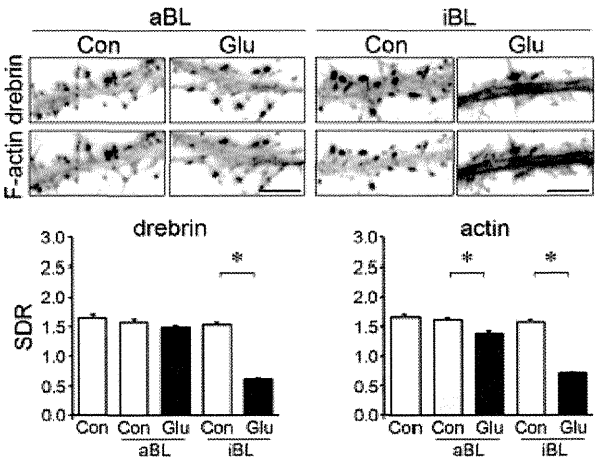

Figure 7. Glutamate-induced DA-actin exodus is blocked by an inhibitor of myosin II ATPase. Neurons (21 DIV) were preincubated with 100 μM aBL for 30 min and then stimulated with 100 μM glutamate for 10 min. F-actin images indicate that spines kept their structure during the experiment although their shapes were changed. Scale bars, 5 μm. The drebrin SDR of aBL-treated neurons was not decreased by glutamate stimulation (n = 30 cells; p = 0.06, Student's *t* test), although that of iBL-treated neurons was decreased (n = 30 cells; $p<0.01$, Scheffe's test). On the other hand, the actin SDR of aBL-pretreated neurons was slightly, but significantly, decreased by glutamate stimulation (n = 30 cells; $p<0.01$, Scheffe's test), although the reduction was much smaller than that observed in iBL-pretreated neurons (n = 30 cells; $p<0.01$, Student's *t* test). Error bars represent s.e.m.

doi:10.1371/journal.pone.0085367.g007

Because MLCK and ROCK phosphorylate MLC [33], the above data suggest that MLC phosphorylation is not involved in the DA-actin exodus.

Discussion

In the present study we demonstrated that (1) chemical long-term potentiation (cLTP) stimulation induces rapid DA-actin exodus and subsequent DA-actin re-entry in dendritic spines, (2) Ca^{2+} influx through NMDA receptors regulates both the exodus and the basal accumulation of DA-actin, and (3) the DA-actin exodus is blocked by a myosin II ATPase inhibitor, but is not blocked by either MLCK or ROCK inhibitors.

These results indicate that Ca^{2+} influx through NMDA receptors induces the DA-actin exodus in LTP induction, and that myosin II mediates the interaction between NMDA receptor activation and DA-actin exodus (Fig. S2). Furthermore, the Ca^{2+} influx seems to activate myosin II ATPase by a rapid actin-linked mechanism instead of slow MLC phosphorylation. Thus the myosin II-mediated DA-actin exodus might be an initial event in LTP induction, triggering actin polymerization and spine enlargement.

SDR analysis of DA-actin migration in and out of dendritic spines

In the present study, using drebrin SDR, we found that APV treatment not only inhibits the DA-actin exodus but also facilitates the accumulation of DA-actin in dendritic spines. In our previous studies, we could not detect any facilitative effect of APV treatment on drebrin accumulation in dendritic spines, because we used drebrin cluster density along dendrites for assessing the dynamic changes in drebrin localization [13,17]. Although this method is sensitive enough to detect the loss of drebrin from

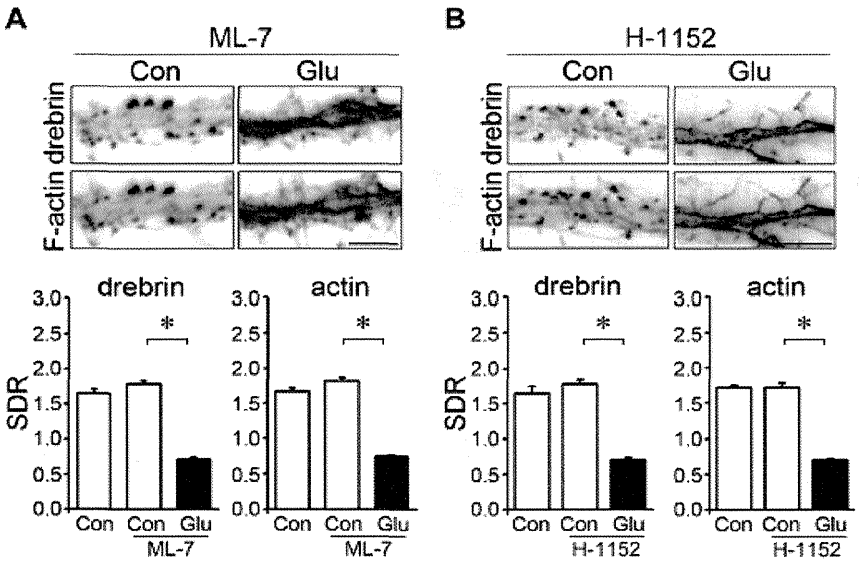

Figure 8. The DA-actin exodus is not blocked by inhibitors of myosin light chain kinase (MLCK) or Rho-associated kinase (ROCK). Neurons (21 DIV) were preincubated with 10 μM of ML-7, an inhibitor of MLCK (A) or 1 μM H-1152, an inhibitor of ROCK (B) for 30 min, and then stimulated with 100 μM glutamate for 10 min. Neither ML-7 (n = 30 cells; drebrin SDR $p<0.01$, actin SDR $p<0.01$, Scheffe's test) nor H1152 (n = 30 cells; drebrin SDR $p<0.01$, actin SDR $p<0.01$, Scheffe's test) blocked the DA-actin exodus. F-actin images indicate that spines kept their structure during the experiment although their shapes were changed. Scale bars, 5 μm.

doi:10.1371/journal.pone.0085367.g008

dendritic spines, it is not sensitive enough to detect the accumulation of drebrin in dendritic spines.

By comparing the changes in drebrin and actin SDRs we can extrapolate the changes in non-DA-actin, because the total F-actin shown by the actin SDR consists of DA-actin and non-DA-actin. In the present study we found that the glutamate-induced exoduses of DA-actin and non-DA-actin are differentially regulated by each glutamate receptor subtype. Thus measurement of SDR is a useful method to analyze the migration of proteins in and out of dendritic spines.

The DA-actin exodus may trigger the facilitation of F-actin polymerization in dendritic spines

After NMDA receptor activation in LTP induction, facilitation of actin polymerization and spine enlargement are observed [34–35]. However, the underlying mechanisms of these processes have not been elucidated. The present study shows that the total amount of F-actin in dendritic spines transiently decreases shortly after cLTP stimulation, resulting from a DA-actin exodus. Once the total F-actin in dendritic spines reduces by the DA-actin exodus, monomeric actin is likely to immediately refill the vacant space by diffusion [15]. The increase in the amount of monomeric actin is known to facilitate F-actin polymerization [36]. In addition, the treadmilling rate of DA-actin is low [8], suggesting that the high level of DA-actin in dendritic spines makes the average treadmilling rate of total F-actin lower in resting dendritic spines. Because quickly-treadmilling non-DA-actin predominates in dendritic spines after the DA-actin exodus, the average treadmilling rate of total F-actin is increased. Together, it is indicated that the DA-actin exodus increases the monomeric actin content and the treadmilling rate of F-actin in dendritic spines, resulting in the facilitation of F-actin polymerization and spine enlargement (Fig. S2).

Possible molecular mechanism for how Ca^{2+} influx activates myosin II ATPase in dendritic spines

Myosin II ATPase is known to be activated by MLC phosphorylation or by an actin-linked mechanism. The important issue remaining is which molecular mechanism is related to the DA-actin exodus. MLCK and ROCK are two major candidates for the regulator of MLC phosphorylation [33]. The present study reveals that block of neither MLCK nor ROCK inhibits the DA-actin exodus. This finding suggests that MLC phosphorylation is not involved in the DA-actin exodus.

Thus activation of myosin II ATPase by an actin-linked mechanism is likely involved in the DA-actin exodus. In the actin-linked mechanism, myosin II ATPase is activated by the release of the suppressed actomyosin interaction. In mammalian skeletal muscles, when Ca^{2+} binds to the troponin complex, the actomyosin interaction suppressed by tropomyosin is released, and consequently myosin II ATPase is activated. Because drebrin A inhibits the myosin II ATPase activity similar to tropomyosin [20], drebrin A is thought to be the counterpart of tropomyosin in dendritic spines [14]. Therefore it is suggested that drebrin A protects actin filaments from the interaction with myosin II in the resting dendritic spines, resulting in the inhibition of myosin II ATPase. Once NMDA receptors are activated, the Ca^{2+} influx through NMDA receptors may change the location of drebrin A on the actin filaments, releasing the actomyosin interaction suppressed by drebrin A. Consequently myosin II ATPase is activated in dendritic spines. Thus myosin II ATPase activation by an actin-linked mechanism may be an underlying molecular mechanism for the DA-actin exodus.

Furthermore, the present data shows that the DA-actin exodus occurs immediately after cLTP stimulation. The activation of myosin II ATPase by an actin-linked mechanism occurs within 20 ms after stimulation [37]. Thus the myosin-II mediated DA-actin exodus might be an initial event in LTP induction, triggering actin polymerization and spine enlargement.

Role of DA-actin re-entry into dendritic spines

DA-actin re-entry follows the DA-actin exodus. In the present study we found that the LTP-induced DA-actin exodus triggers F-actin polymerization and spine enlargement. The DA-actin re-entry may be related to maintenance of LTP. After the DA-actin re-entry, the dynamic and stable F-actin pools are probably reestablished in the dendritic spines. As a result, polymerization and depolymerization of F-actin is balanced in dendritic spines and the enlarged spine morphology is maintained (Fig. S2). In fact, long lasting increases in F-actin and drebrin content in dendritic spines have been reported when LTP is maintained *in vivo* [38].

What are the underlying mechanisms of DA-actin re-entry? Reduction of the Ca^{2+} influx into dendritic spines might induce the DA-actin re-entry, because the basal accumulation of DA-actin is negatively regulated by Ca^{2+} influx through NMDA receptors and voltage-dependent Ca^{2+} channels in resting spines. Another possible mechanism is a signaling cascade linked to AMPA receptors. LTP stimulation is known to increase the AMPA receptor density in dendritic spines [39]. Because AMPA receptor activity facilitates accumulation of DA-actin in the dendritic spines of immature neurons [17], AMPA receptors might also be involved in the DA-actin re-entry in mature neurons.

Supporting Information

Figure S1 Effects of glutamate stimulation on the density of spines and presynaptic terminals. (**A**) DiI staining of hippocampal neurons. Fixed cultures on coverslips were bathed in PBS and placed on the stage of an inverted phase microscope. Individual cells were stained with 1,1′-dioctadecyl-3,3,3′,3′-tetramethylindocarbocyanine perchlorate (**DiI**; Molecular Probes, Inc., Eugene, OR). The DiI was dissolved in vegetable oil to saturation, loaded into a glass micropipette (Eppendorf), and applied by pressure ejection onto the multipolar neurons. The coverslips were then placed at room temperature in small petri dishes containing PBS. After 12–24 h, which allowed for sufficient transport of the dye, cells were examined by fluorescence microscopy. The spine morphology of boxed areas in upper panels are shown at higher magnification in middle panels. Note that the spines kept their structures during the experiment. Scale bars, 10 μm. Left panel in the bottom shows the density of dendritic spines. To measure spine density, the number of spines per cell was then counted for 25 cells (50–100 μm total dendritic length per neuron). Significant differences were not observed between the control (n = 42 dendrites) and glutamate-treated dendrites (n = 44 dendrites; p = 0.73, Student's t test). Bar graphs represent dendritic spine density. The cumulative frequency plots in the bottom show distribution of spine length and spine width. The glutamate treatment significantly increased the spine length (control, 1.39±0.03 μm, n = 42 dendrites; glutamate, 1.72±0.05 μm, n = 44 dendrites, p<0.01, Student's t test) and reduced the spine width (control, 0.96±0.01 μm, n = 42 dendrites; glutamate, 0.82±0.02 μm, n = 44 dendrites, p<0.01, Student's t test). (**B**) Triple-labeled images of drebrin, F-actin and synapsin I in hippocampal neurons. Scale bars, 10 μm. (**C**) Bar graphs represent the density of synapsin I clusters. Synapsin I cluster density was measured according to previously described methods

(Takahashi et al., 2009). No significant differences in the density of synapsin I clusters were detected between control (n = 30 dendrites) and glutamate-stimulated neurons (n = 30 dendrites; p = 0.86, Student's t test). Data are presented as mean ± s.e.m.
(TIF)

Figure S2 Model for architectural changes in the actin cytoskeleton during LTP formation. (**A**) Dendritic spines in the resting state contain a dynamic F-actin pool (non-DA-actin) at the tip of the spine head, and a stable pool (DA-actin) in the base of the spine head. Although the dynamic F-actin pool shows quick treadmilling, polymerization and depolymerization of F-actin is balanced, consequently maintaining spine morphology. (**B**) Once Ca^{2+} enters through NMDA receptors, it activates myosin II ATPase through disinhibition of the DA-actin and myosin-II interaction. Consequently DA-actin exits the dendritic spine head and simultaneously monomeric actin refills the vacant space in the spine head. Both these changes cooperate to facilitate the polymerization of non-DA-actin, which is the predominant component of an enlargement F-actin pool in the spine head. Accordingly the spine head is enlarged. (**C**) Ca^{2+} reduction and/or APMA receptor activation induce DA-actin re-entry. The DA-actin re-entry reconstitutes the dynamic and stable F-actin pools in dendritic spines, contributing to maintenance of the enlarged spine morphology until the next DA-actin exodus is triggered.
(EPS)

Acknowledgments

We thank Drs. Kenji Hanamura and Mitsuyoshi Saito for helpful discussions and Ms. Tomoko Takahashi for technical assistance.

Author Contributions

Conceived and designed the experiments: TM YS TS. Performed the experiments: TM HY YI HT. Analyzed the data: TM YS HY YI HT NK MK. Wrote the paper: TM YS TS.

References

1. Shirao T, Kojima N, Nabeta Y, Obata K (1989) Two forms of drebrins, developmentally regulated brain proteins, in rat. Proc Japan Acad 65: 169–172.
2. Ishikawa R, Hayashi K, Shirao T, Xue Y, Takagi T, et al. (1994) Drebrin, a development-associated brain protein from rat embryo, causes the dissociation of tropomyosin from actin filaments. J Biol Chem 269: 29928–29933.
3. Aoki C, Sekino Y, Hanamura K, Fujisawa S, Mahadomrongkul V, et al. (2005) Drebrin A is a postsynaptic protein that localizes in vivo to the submembranous surface of dendritic sites forming excitatory synapses. J Comp Neurol 483: 383–402.
4. Grintsevich EE, Galkin VE, Orlova A, Yuterberg AJ, Mikati MM, et al. (2010) Mapping of drebrin binding site on F-actin. J Mol Biol 398: 542–554.
5. Sharma S, Grintsevich EE, Phillips ML, Reisler E, Ginzewski JK (2011) Atomic force microscopy reveals drebrin induced remodeling of f-actin with subnanometer resolution. Nano Lett 11: 825–827.
6. Asada H, Uyemura K, Shirao T (1994) Actin-binding protein, drebrin, accumulates in submembranous regions in parallel with neuronal differentiation. J Neurosci Res 38: 149–159.
7. Mizui T, Kojima N, Yamazaki H, Katayama M, Hanamura K, et al. (2009) Drebrin E is involved in the regulation of axonal growth through actin-myosin interactions. J Neurochem 109: 611–622.
8. Mikati MA, Grintsevich EE, Reisler E (2013) Drebrin-induced Stabilization of Actin Filaments. J Biol Chem 288: 19926–19938.
9. Takahashi H, Sekino Y, Tanaka S, Mizui T, Kishi S, et al. (2003) Drebrin-dependent actin clustering in dendritic filopodia governs synaptic targeting of postsynaptic density-95 and dendritic spine morphogenesis. J Neurosci 23: 6586–6595.
10. Worth DC, Daly CN, Geraldo S, Oozeer F, Gordon-Weeks PR (2013) Drebrin contains a cryptic F-actin-bundling activity regulated by Cdk5 phosphorylation. J Cell Biol 202: 793–806.
11. Honkura N, Matsuzaki M, Noguchi J, Ellis-Davies GC, Kasai H (2008) The subspine organization of actin fibers regulates the structure and plasticity of dendritic spines. Neuron 57: 719–729.
12. Shirao T, González-Billault C (2013) Actin filaments and microtubules in dendritic spines. J Neurochem 126: 155–164.
13. Sekino Y, Tanaka S, Hanamura K, Yamazaki H, Sasagawa Y, et al. (2006) Activation of N-methyl-D-aspartate receptor induces a shift of drebrin distribution: Disappearance from dendritic spines and appearance in dendritic shafts. Mol Cell Neurosci 31: 493–504.
14. Sekino Y, Kojima N, Shirao T (2007) Role of actin cytoskeleton in dendritic spine morphogenesis. Neurochem Int 51: 92–104.
15. Star EN, Kwiatkowski DJ, Murthy VN (2002) Rapid turnover of actin in dendritic spines and its regulation by activity. Nat Neurosci 5: 239–246.
16. Ikeda J, Inoue A, Ito H, Okabe S (2005) Bi-directional regulation of postsynaptic cortactin distribution by BDNF and NMDA receptor activity. Eur J Neurosci 22: 2985–2994.
17. Takahashi H, Yamazaki H, Hanamura K, Sekino Y, Shirao T (2009) AMPA receptor inhibition causes abnormal dendritic spines by destabilizing drebrin. J Cell Sci 122: 1211–1219.
18. Rex CS, Gavin CF, Rubio MD, Kramar EA, Chen LY, et al. (2010) Myosin IIb regulates actin dynamics during synaptic plasticity and memory formation. Neuron 67: 603–617.
19. Cheng XT, Hayashi K, Shirao T (2000) Non-muscle myosin IIB-like immunoreactivity is present at the drebrin-binding cytoskeleton in neurons. Neurosci Res 36: 167–173.
20. Hayashi K, Ishikawa R, Ye LH, He XL, Takata K, et al. (1996) Modulatory role of drebrin on the cytoskeleton within dendritic spines in the rat cerebral cortex. J Neurosci 16: 7161–7170.
21. Murrell MP, Gardel ML (2012) F-actin buckling coordinates contractility and severing in a biomimetic actomyosin cortex. Proc Natl Acad Sci USA 109: 20820–20825.
22. Lu W, Man H, Ju W, Trimble WS, MacDonald JF, et al. (2001) Activation of synaptic NMDA receptors induces membrane insertion of new AMPA receptors and LTP in cultured hippocampal neurons. Neuron 29: 243–254.
23. Shirao T, Obata K (1986) Immunochemical homology of 3 developmentally regulated brain proteins and their developmental change in neuronal distribution. Brain Res 394: 233–244.
24. Swayze RD, Lise MF, Levinson JN, Phillips A, El-Husseini A (2004) Modulation of dopamine mediated phosphorylation of AMPA receptors by PSD-95 and AKAP79/150. Neuropharmacology 47: 764–778.
25. Hayashi K, Shirao T (1999) Change in the shape of dendritic spines caused by overexpression of drebrin in cultured cortical neurons. J Neurosci 19: 3918–3925.
26. Xie H (1984) Differences in the Efficiency and Stability of Gene Expression after Transfection and Nuclear Injection: A Study with a Chick δ-Crystallin Gene. Cell Struct Funct 8: 315–325.
27. Hanamura K, Mizui T, Kakizaki T, Roppongi RT, Yamazaki H, et al. (2010) Low accumulation of drebrin at glutamatergic postsynaptic sites on GABAergic neurons, Neuroscience 169: 1489–1500.
28. Kaech S, Banker G (2006) Culturing hippocampal neurons, Nat Protoc 1: 2406–2415.
29. Xie Z, Srivastava DP, Photowala H, Kai L, Cahill ME, et al. (2007) Kalirin-7 controls activity-dependent structural and functional plasticity of dendritic spines. Neuron 56: 640–656.
30. Ryu J, Liu L, Wong TP, Wu DC, Burette A, et al. (2006) A critical role for myosin IIb in dendritic spine morphology and synaptic function. Neuron 49: 175–182.
31. Hardingham GE, Fukunaga Y, Bading H (2002) Extrasynaptic NMDARs oppose synaptic NMDARs by triggering CREB shut-off and cell death pathways. Nat Neurosci 5: 405–414.
32. Yuste R, Majewska A, Holthoff K (2000) From form to function: calcium compartmentalization in dendritic spines. Nat Neurosci 3: 653–659.
33. Matsumura F (2005) Regulation of myosin II during cytokinesis in higher eukaryotes. Trends Cell Biol 15: 371–377.
34. Matsuzaki M, Honkura N, Ellis-Davies GC, Kasai H (2004) Structural basis of long-term potentiation in single dendritic spines. Nature 429: 761–766.
35. Okamoto K, Nagai T, Miyawaki A, Hayashi Y (2004) Rapid and persistent modulation of actin dynamics regulates postsynaptic reorganization underlying bidirectional plasticity. Nat Neurosci 7: 1104–1112.
36. Korn ED, Carlier MF, Pantaloni D (1987) Actin polymerization and ATP hydrolysis. Science 238: 638–644.
37. Konishi M (1998) Cytoplasmic free concentrations of Ca^{2+} and Mg^{2+} in skeletal muscle fibers at rest and during contraction. Jpn J Physiol 48: 421–438.
38. Fukazawa Y, Saitoh Y, Ozawa F, Ohta Y, Mizuno K, et al. (2003) Hippocampal LTP is accompanied by enhanced F-actin content within the dendritic spine that is essential for late LTP maintenance in vivo. Neuron 38: 447–460.
39. Lynch MA (2004) Long-term potentiation and memory. Physiol Rev 84: 87–136.

ACS Chemical Neuroscience

Research Article

pubs.acs.org/acschemicalneuroscience

Discovery of a Tamoxifen-Related Compound that Suppresses Glial L-Glutamate Transport Activity without Interaction with Estrogen Receptors

Kaoru Sato,*[,‡,†] Jun-ichi Kuriwaki,[‡,†] Kanako Takahashi,[‡] Yoshihiko Saito,[§] Jun-ichiro Oka,[§] Yuko Otani,[∥] Yu Sha,[∥] Ken Nakazawa,[‡] Yuko Sekino,[‡] and Tomohiko Ohwada*[,∥]

[‡]Division of Pharmacology, National Institute of Health Sciences, 1-18-1 Kamiyoga, Setagaya-ku, Tokyo 158-8501, Japan

[§]Laboratory of Pharmacology, Faculty of Pharmaceutical Sciences, Tokyo University of Science, 2541 Yamazaki, Noda-city, Chiba 278-8510, Japan

[∥]Laboratory of Organic and Medicinal Chemistry, Graduate School of Pharmaceutical Sciences, University of Tokyo, 7-3-1, Hongo, Bunkyo-ku, Tokyo 113-0033, Japan

ABSTRACT: We recently found that tamoxifen suppresses L-glutamate transport activity of cultured astrocytes. Here, in an attempt to separate the L-glutamate transporter-inhibitory activity from the estrogen receptor-mediated genomic effects, we synthesized several compounds structurally related to tamoxifen. Among them, we identified two compounds, **1** (YAK01) and **3** (YAK037), which potently inhibited L-glutamate transporter activity. The inhibitory effect of **1** was found to be mediated through estrogen receptors and the mitogen-activated protein kinase (MAPK)/phosphatidylinositol 3-kinase (PI3K) pathway, though **1** showed greatly reduced transactivation activity compared with that of 17β-estradiol. On the other hand, compound **3** exerted its inhibitory effect through an estrogen receptor-independent and MAPK-independent, but PI3K-dependent pathway, and showed no transactivation activity. Compound **3** may represent a new platform for developing novel L-glutamate transporter inhibitors with higher brain transfer rates and reduced adverse effects.

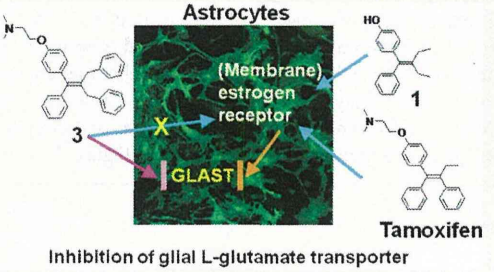

KEYWORDS: *Tamoxifen, astrocyte, L-glutamate transporter, ERα, tetrasubstituted ethylene, nongenomic pathway*

L-Glutamate (L-Glu) is one of the major excitatory neurotransmitters in the central nervous system (CNS), but high concentrations of extracellular L-Glu cause excessive stimulation of L-Glu receptors in the CNS, leading to neurotoxicity.[1,2] Astrocyte L-Glu transporters are the only machinery available to remove L-Glu from extracellular fluid and to maintain a low and nontoxic concentration of L-Glu.[3] Consequently, dysfunction of astrocyte L-Glu transporters is considered to be implicated in the pathology of neurodegenerative conditions.[4] Therefore, exogenous compounds that can regulate the function of L-Glu transporters may provide chemical tools to investigate the regulatory mechanisms of these transporters at the molecular level, and would also be candidate therapeutic agents.

There is growing evidence that estrogen receptor (ER) α, which is a nuclear ER (nER) that mediates genomic effects, can also be translocated to plasma membranes and mediate acute nongenomic effects in some cases. We have clarified that 17β-estradiol (E2) inhibits L-Glu transporters via a nongenomic pathway involving membrane-associated ERα (mERα).[5] Tamoxifen (Tam), a synthetic estrogen analogue that is clinically used in the treatment of breast cancer to block the proliferative action of estrogens,[6] also inhibited astrocyte L-Glu transporters at picomolar concentration, probably through the same nongenomic pathway as E2.[7] Because overexpression of astrocyte L-Glu transporters is often associated with neuropsychiatric disorders,[4] inhibitors of L-Glu transporters may be clinically useful to ameliorate these disorders.[8] However, Tam also acts on genomic pathways involving nuclear estrogen receptors (nERs) α and β, depending on the cell type and promoter context,[9] and so may cause adverse effects including endometrial changes, depression and weight gain.[10,11] Therefore, Tam-inspired compounds that retain the inhibitory effect on L-Glu transporters, but lack the nER-mediated genomic effects, would be useful tools for biological research, as well as candidate therapeutic agents.

Tam is a tetrasubstituted triphenylethylene derivative, in which the four substituents on the olefinic carbon atoms are different. This structural complexity makes the stereospecific synthesis of Tam-related derivatives difficult. We thus focused on Tam-inspired compounds bearing identical substituents on at least one of the olefinic carbon atoms.[12] It is well-known that the *N*,*N*-dimethylaminoethyl substituent on the phenolic oxygen atom and the regiochemistry of the tetrasubstituted olefin of Tam are crucial for ER binding activity.[13] So, we

Received: September 29, 2011
Accepted: November 14, 2011

considered that more symmetrical derivatives of Tam might show reduced ER-binding ability.

Among our synthesized compounds, we found two, compounds **1** (YAK01) and **3** (YAK037), with potent L-Glu transporter-inhibitory activity. Studies of their mechanisms of action indicated that, unlike Tam, compound **3** acts through an ER-independent and MAPK-independent, but PI3K-dependent pathway and shows no transactivation activity for nERs. We believe this compound may represent a new platform for developing novel L-Glu transporter inhibitors with higher brain transfer rates and reduced adverse effects.

■ RESULTS AND DISCUSSION

We synthesized several Tam-inspired compounds bearing identical substituents on one carbon atom of the olefin,[12] and found that two of them were potent inhibitors of astrocyte L-Glu transporters. The diethyl-substituted derivative **1** inhibited L-Glu transporters in the picomolar range (62.7 ± 7.48% of control at 1 pM; Figure 2A). The dose–response curve for the inhibitory activity was not linear, but followed an inverted U-shaped curve; however, such a non-monotonic dose dependence is rather common for hormones and their mimetics.[16] On the other hand, when the symmetrical substituent was changed from ethyl to benzyl (**2**), the inhibitory effect was lost (Figure 2B). However, when the phenolic oxygen atom of **1** was substituted with a *N*,*N*-dimethylaminoethyl group (Figure 1C), we found

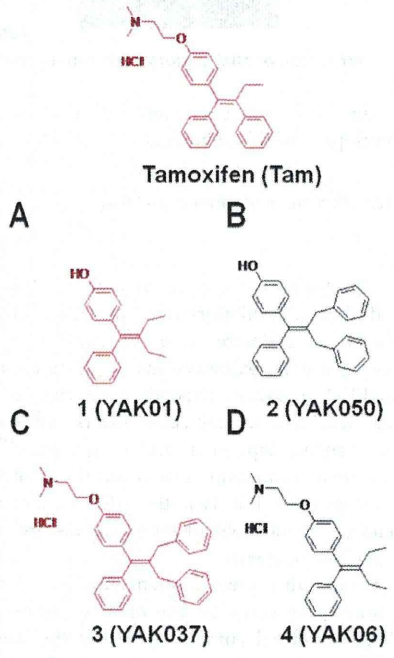

Figure 1. Chemical structures of the newly synthesized tamoxifen-related compounds.

that the resulting compound **3** showed dose-dependent L-Glu transporter inhibition in the picomolar range (63.8 ± 5.49% of control at 1 pM; Figure 2C). The dose-dependency of the effect of **3** suggested that the underlying mechanism might be different from that in the case of **1**. Compound **4** was inactive (Figure 2D).

We next examined the effects of **1** and **3** on cell viability by means of MTT reduction assay and LDH leakage assay, using the same cultured sample. Neither of the compounds was cytotoxic at concentrations below 1 μM (Figure 3), though 100 μM **1** and 10 μM **3** caused severe cell damage. These results exclude the possibility that the L-Glu clearance-inhibitory effects of these compounds at concentrations below 1 μM were caused by cell damage.

In order to confirm the involvement of L-Glu transporters in the inhibition of L-Glu uptake by our compounds, and to rule out the possibility that **1** and **3** act by inducing L-Glu release from astrocytes, we next examined the effect of **1** and **3** on L-Glu clearance when the L-Glu transporter activity was blocked with TBOA, a potent nonselective L-Glu transporter inhibitor (IC_{50}: 48 μM for GLAST/EAAT1, 7 μM for GLT1/EAAT2). We confirmed that application of 1 mM TBOA potently inhibited L-Glu transporter activity; that is, TBOA caused reversible chemical knock-down of L-Glu transporter activity.[7] When either **1** or **3** was coapplied with 1 mM TBOA, these compounds no longer influenced L-Glu clearance (Figure 4), indicating that the actions of these compounds are indeed mediated by L-Glu transporters, and do not involve L-Glu release from astrocytes.

Our cultured astrocytes predominantly expressed ERα, and little or no expression of ERβ was detected.[5] Tam is known to be a partial agonist of ERs,[9] raising the possibility that the compounds exerted their inhibitory effects via interaction with ERα. Therefore, we examined the involvement of ERα by coapplication of ICI182,780, a high-affinity antagonist of ERs. ICI182,780 dose-dependently blocked the inhibition of L-Glu uptake caused by **1** (Figure 5A) at 0.01, 0.1, and 1 μM, at which the effects of Tam were reported to be completely suppressed.[7] In contrast, ICI182,780 had no effect on the inhibition by **3** (Figure 5B), suggesting that the mechanism of the inhibition by **3** is independent of ERs. We further examined the signal transduction pathways mediating the effects of **1** and **3**. When coapplied with U0126, which inhibits mitogen-activated protein kinase/extracellular signal-regulated kinase 1 (MEK1, IC50: 70 nM) and MEK2 (IC50: 60 nM), the inhibitory effect by **1** was blocked, whereas that of **3** was not (Figure 6A). On the other hand, when coapplied with LY294002, a specific phosphoinositide 3-kinase (PI3K) inhibitor (IC50: 70 nM), the inhibitory effects of both compounds were completely blocked (Figure 6B). These results suggest that PI3K is a common mediator of the effects of both compounds, whereas mitogen-activated protein kinase (MAPK) is involved only in the mechanism of inhibition by **1**.

Finally we examined the ER-agonist potency of **1** and **3**, i.e., the transcriptional effects of these compounds via human ERα and ERβ, using HEK293/hERα and HEK293/hERβ reporter cells (Figure 7). Compound **1** showed agonist activity in both of 293/hERα and 293/hERβ reporter cells, though the binding affinities were much weaker than that of E2. The EC50 values of **1** for ERα and ERβ are 30.8 nM and 10.4 nM, respectively (1.25 nM and 0.864 nM, respectively, for E2). The relative agonist activity of **1** was 66.8% of that of E2 in HEK293/hERα and 122.0% of that of E2 in HEK293/hERβ. Strikingly, **3** showed no agonist potency for ERα or ERβ. These findings strongly suggest that **3** can inhibit L-Glu transporters without interaction with ERs.

In this study, we examined the potential of Tam-related compounds to inhibit GLAST/EAAT1 and GLT1/EAAT2, which are major astrocytic L-Glu transporters in the rat

dx.doi.org/10.1021/cn200091w | ACS Chem. Neurosci. XXXX, XXX, XXX–XXX

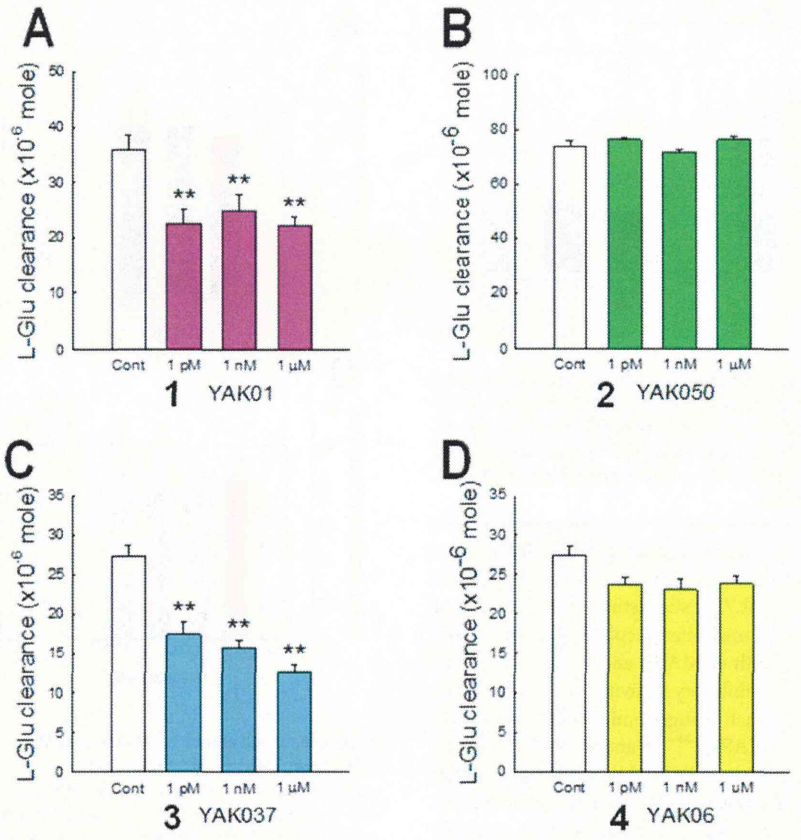

Figure 2. Compounds **1** and **3** inhibited L-Glu clearance in cultured astrocytes. The open column shows the control clearance, and colored columns show the clearance in the presence of various concentrations of compounds **1** (A), **2** (B), **3** (C), and **4** (D). $^{**}p < 0.01$ vs control group ($N = 6$), Tukey's test following ANOVA.

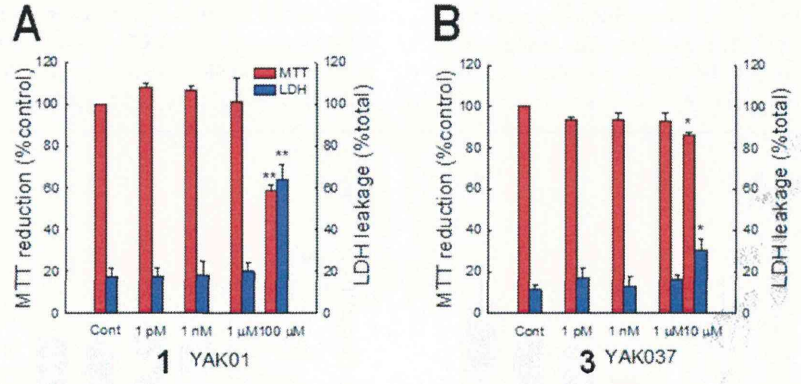

Figure 3. Effects of compounds **1** and **3** on cell viability. The results of MTT reduction and LDH leakage assays of **1** (A) and **3** (B) are shown. $^{*}p < 0.05$, $^{**}p < 0.01$ vs control group ($N = 6$), Tukey's test following ANOVA.

forebrain. Although GLT-1 is the main regulator of synaptically released L-Glu ~~in vivo~~, the predominant subtype changes to GLAST in cultured astrocytes, possibly owing to the lack of interaction of astrocytes with neurons.[17] We confirmed that GLAST is the main functional L-Glu transporter in our primary-cultured astrocytes by Western blotting and pharmacological experiments (data not shown), in accordance with a previous report.[18] Therefore, the effects of the compounds observed here can be interpreted as being due to modulation of GLAST functional activity.

There is growing evidence that ERα, which is a nER that mediates genomic effects, can also be translocated to plasma membranes and mediate acute nongenomic effects in some cases. Transfection of CHO cells with nERs was reported to result in ER expression in both nuclei and membranes.[19] ERs on the plasma membranes of tumor cells were demonstrated to be structurally similar to nERs.[20] Further, mERα activated metabotropic glutamate receptor 5 (mGluR5) in striatal neurons in the CNS.[21] In our previous study, we clarified that the predominant ER subtype in cultured astrocytes was ERα, and

dx.doi.org/10.1021/cn200091w | ACS Chem. Neurosci. XXXX, XXX, XXX–XXX

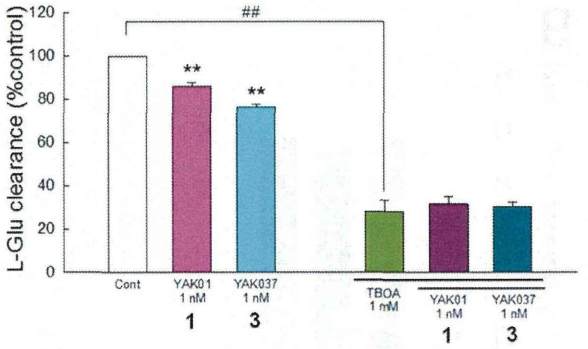

Figure 4. Compounds **1** and **3** suppressed L-Glu clearance in astrocyte culture by decreasing the functional activity of L-Glu transporter. L-Glu clearance in the presence and absence of compounds **1** and **3** is shown, together with their effects in the copresence of the potent nonselective L-Glu transporter inhibitor TBOA. $^{**}p < 0.01$ vs control group ($N = 6$), Tukey's test following ANOVA.

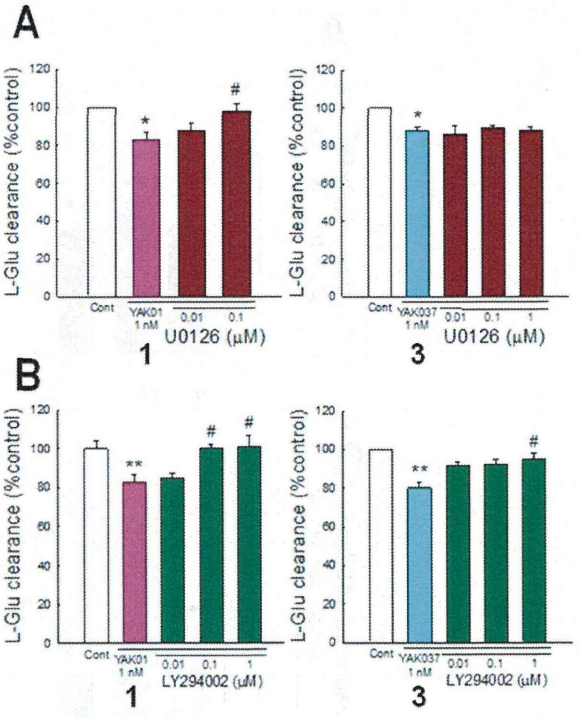

Figure 6. Involvement of MAPK and PI3K in the L-Glu transporter-inhibitory activity of compounds **1** (A) and **3** (B). Effects of compounds **1** (left panels) and **3** (right panels) on L-Glu clearance in the presence and absence of various concentrations of U0126, an inhibitor of MAPK/ERKs (A) or LY294002, a specific inhibitor of PI3K (B). $^{*}P < 0.05$, $^{**}p < 0.01$ vs control group, $\#p < 0.05$ vs compound-treated group ($N = 6$), Tukey's test following ANOVA.

184 estrogens (such as E2 and Tam) inhibited L-Glu transporter
185 activity via the activation of mERα.[5] We found that the effects
186 of **1** were blocked by ICI182,780, suggesting an interaction of
187 **1** with ERα. In addition, our pharmacological experiments
188 showed that activation of both of MAPK and PI3K is necessary
189 for the L-Glu transporter-inhibitory activity of **1**. There are
190 many reports indicating that nongenomic effects involving
191 mERα are mediated via MAPK [21−23] and PI3K.[22,24] Taken
192 together, the effects of **1** may be mediated by mERα in a similar
193 manner to E2 and Tam. E2 was reported to activate MAPK via
194 both PI3K-dependent and independent pathways in a single
195 neuron.[22] Whether or not the same signaling pathways also
196 exist in astrocytes is not yet known. It is of interest that other
197 studies have found that estrogens also inhibit dopamine
198 transporter (DAT) through the activation of mERα.[25,26]
199 On the other hand, the effect of **3** was ER-independent and
200 MAPK-independent, but PI3K-dependent. Our binding assay
201 revealed that **1** binds with ERs, but **3** does not. Based on these
202 results, we propose that the mechanisms of the L-Glu
203 transporter-inhibitory effects of **1** and **3** are different, as
204 illustrated in Figure 8. The effect of **3** was possibly mediated by
205 GPR30, a newly found ER, which is suggested to mediate the
206 rapid nongenomic effects of estrogens.[27,28] In the case of
207 GPR30, ICI182,780 acts as agonist, leading to activation of

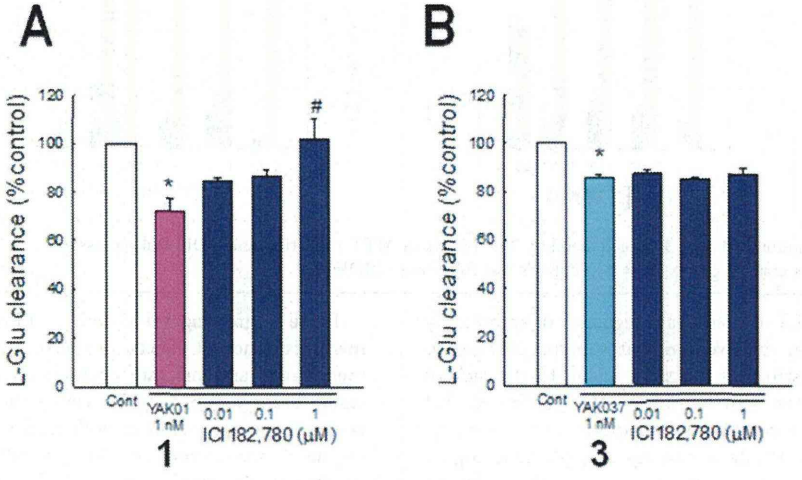

Figure 5. Involvement of ERs in the L-Glu transporter-inhibitory effects of compounds **1** and **3**. Effects of compounds **1** (A) and **3** (B) on L-Glu clearance in the presence and absence of various concentrations of ICI182,780, a high-affinity antagonist of ERs. $^{*}P < 0.05$ vs control group, $\#p < 0.05$ vs compound-treated group ($N = 6$), Tukey's test following ANOVA.

dx.doi.org/10.1021/cn200091w | ACS Chem. Neurosci. XXXX, XXX, XXX–XXX